https://doi.org/10.15255/KUI.2023.040
KUI-10/2024
Original scientific paper
Received September 29, 2023
Accepted November 29, 2023

Effect of NaX Zeolite Mass and Baffle Presence on Copper Sorption

A. Herceg,[a] *A. Bašić*,[a*] *Ž. Penga*,[b] and *S. Sviloviće*[a]

[a] University of Split, Faculty of Chemistry and Technology, Ruđera Boškovića 35, 21 000 Split, Croatia
[b] University of Split, Faculty of Electrical Engineering, Mechanical Engineering and Naval Architecture, Ruđera Boškovića 32, 21 000 Split, Croatia

4th ZORH CONVENTION

Abstract

Sorption is often conducted in stirred batch reactors without assessing the impact of mixing on yield and costs. Operating the mixing in the batch reactor at a state of complete suspension, *i.e.*, at just suspended impeller speed, N_{JS}, is a compromise between these conflicting goals. Therefore, copper sorption on NaX zeolite using a pitched blade turbine was conducted in both baffled and unbaffled batch reactors at N_{JS}. Maintaining constant impeller to reactor diameter ratio ($D/d_T = 0.32$), and impeller off-bottom clearance ($C/H = 0.33$), kinetic sorption experiments were performed. Besides kinetic sorption experiments and the kinetic analysis of data obtained, to gain insight into the hydrodynamic behaviour of the system, transient multiphase computational fluid dynamics simulations (CFD) were performed. The N_{JS} speed is related to the particle settling speed, wherein a higher zeolite suspension mass concentration requires a greater N_{JS} speed, resulting in increased energy consumption. The differences in N_{JS} speeds for the investigated zeolite suspension mass concentrations were found to be insubstantial, and therefore, the increase in mixing intensity for the tested systems was not deemed significant. Regardless of the zeolite mass used, the values of N_{JS} and P_{JS} (mixing power consumption) were consistently higher in the unbaffled reactor. The hydrodynamic conditions employed were found to have no significant effect on the maximum amount of copper sorbed or process efficiency, but was significantly affected by zeolite mass. The kinetics were affected by both, and, generally, sorption occurred faster in the unbaffled reactor.

Keywords

Sorption kinetics, copper, zeolite mass concentration, baffles, CFD

1 Introduction

Zeolites are hydrated aluminosilicates, natural or synthetically produced, whose properties can be designed during synthesis or before use. They are mainly used in industry as molecular sieves, sustainable catalysts, and sorbents.[1,2]

Heavy metal contamination poses a serious environmental issue as metals concentrate in the environment, endangering human health due to their inability to dissolve into benign end products. The toxic activity of heavy metals has been evident since the late nineteenth century, prompting concerns about their adverse effects on humans and other life forms. Human-generated heavy metal-bearing wastewater has gained attention as a key pollution source, necessitating thorough treatment before discharge. This has led to substantial efforts to enhance heavy metal removal processes, such as sorption, coagulation-flocculation, membrane separation, precipitation, electrocoagulation, flotation, and remediation.[3,4] Sorption is a highly successful and cost-effective technology that uses various types of sorbents to remove pollutants.[3–9] The sorption process using zeolite is generally conducted in either a packed bed reactor or a batch reactor.

Previous studies on the kinetics of the studied process in a batch reactor reveal that, like all heterogeneous processes, its kinetics can be controlled by sorption, film diffusion or intraparticle diffusion.[10,11] The slowest step depends on the relative rates of surface reaction and mass transfer. By using a suitable particle size of the sorbent, the effect of intraparticle diffusion can be avoided regardless of the type of reactor used. If sorption is conducted in a stirred batch reactor, film diffusion can be prevented through appropriate mixing conditions. As sorption is a heterogeneous process, mixing influences both the overall sorption rate and the slowest step. The relative rates of steps in a heterogeneous reaction define whether the process is kinetically or mass transfer-controlled.[10] Moreover, selecting a suitable mixing speed is crucial to completely suspend the solid. Below this speed, the entire particle is not accessible for sorption, leading to accumulation on the reactor bottom, while above this speed result in a slow or negligible increase in the reaction rate .[12] Furthermore, an appropriate mixing speed should result in energy savings and reduced costs while maintaining a satisfactory yield.[13,14] Typically, the just-off-bottom suspension speed, N_{JS}, is employed as an appropriate mixing speed.

The parameters affecting N_{JS} have been extensively researched, revealing that the N_{JS} in solid-liquid systems depends on particle density, particle size, solid mass, and hydrodynamic conditions within the reactor, which in turn depend on its design.[12,15,16] Various types of impellers may be employed to suspend zeolite and generate radial, axial or mixed fluid flow. It has been reported that axial impellers used in reactors with baffles effectively suspend sol-

* Corresponding author: Anita Bašić, Ph.D.
Email: abasic@ktf-split.hr

Note: The findings of this study were presented at the 4th International Convention of Scientists, Specialist Employees, and Students on the topic of Environmental Protection in the Republic of Croatia (4th ZORH Convention), held on April 20–21, 2023, at the Faculty of Chemistry and Technology University of Split, Croatia.

ids.[17,18] However, studies have shown that reactors without baffles generally consume less energy, making them an appealing option for the process industry.[19–22]

The primary focus of the authors investigating the variables influencing sorption was the effects of the initial concentration of the solution, pH values, temperature, type of sorbate, and the sorbent and their ratio. This includes the effect of hydrodynamic conditions in the reactor trough, mixing speed or flow rate, depending on the reactor used.[3,23,24] While the effects of reactor geometry on hydrodynamic conditions and consequently on sorption kinetics, efficiency, and costs did not attract much interest, it was found that reactor geometry indeed affects sorption kinetics, yield, and costs.[25–29]

Therefore, the aim of this work was to analyse the hydrodynamic conditions generated by varying the zeolite mass and the presence of baffles, and to investigate their influence on the kinetics and efficiency of copper sorption. To visualise the hydrodynamic conditions in the reactor, the system's behaviour was simulated using *ANSYS Fluent* v17.2. In addition, a kinetic analysis was performed to determine the slowest step of the process. Two kinetic models were employed to fit the experimental data: the Mixed surface reaction and diffusion controlled adsorption kinetic model (Mixed kinetic model) and Ritchie kinetic model.

2 Experimental

2.1 Materials and reactor design

The copper(II) nitrate solution (Kemika) and NaX zeolite (Alfa Aesar) used in the study were prepared as previously described.[28] The reaction suspensions were prepared by mixing the appropriate mass of the NaX zeolite ($d_p < 90$ µm) and 2.10 dm^3 of the copper(II) nitrate solution ($c_0 = 12.145 \pm 0.112$ mmol dm^{-3}) to obtain a suspension with three different mass concentrations ($\gamma_1 = 5.0$ g dm^{-3}, $\gamma_2 = 7.5$ g dm^{-3}, and $\gamma_3 = 10.0$ g dm^{-3}).

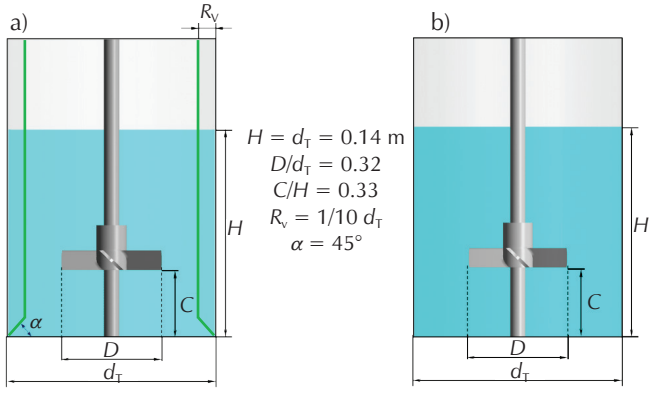

Fig. 1 – Batch reactors: a) baffled reactor, and b) unbaffled reactor

Slika 1 – Šaržni reaktori: a) s razbijalima virova i b) bez razbijala virova

The experiments were conducted in an uncovered batch reactor with a flat bottom, made of glass (Fig. 1). The reactor was placed in a thermostatic bath (Julabo CORIO™ B39) ($T = 298$ K) and equipped with a mechanical stirrer IKA Eurostar 60 Control (IKA-Werke GmbH & Co. KG). A turbine impeller with flat blades inclined at 45° (PBT impeller) was used to agitate the suspension.

2.2 N_{JS}, P_{JS}, and CFD

For each zeolite mass concentration used in both the baffled and unbaffled reactors, the visual Zwietering criteria was employed to determine the impeller speed required for complete suspension.[30] The procedure is described in more detail in the work of *Svilović et al.*[28]

Transient multiphase computational fluid dynamics simulations of the flow in the baffled and unbaffled reactors were conducted using the commercial software *ANSYS Fluent* v17.2 (ANSYS). The Volume of Fluid method was used to approximate the secondary phase. The system torques, τ (N m), at the found N_{JS} were determined.

The determined torque was then used to calculate the mixing power consumption, P_{JS} (W), at complete suspension conditions, as follows:

$$P_{JS} = 2 \cdot \pi \cdot \tau \cdot N_{JS} \quad (1)$$

The finite volume mesh of the reactor, with and without baffles, consisting of stationary and rotating domains, is shown in Figs. 2 and 3. The fluid domain, from which the blades were removed, is a rotating one, while the remaining domain is stationary. The two domains had non-conformal interfaces due to the sliding mesh approach. To improve accuracy, the element sizes between the stationary and rotating domains were selected so that the element sizes at the interfaces would increase at a rate of less than 20 %. To eliminate errors, the fluid domain near the baffles was adjusted to obtain element sizes similar to those found elsewhere.

The rotating domains for the configurations (Figs. 2c and 3c) were composed of four bodies. For different setups, the grid size and the size of the time steps were thoroughly evaluated. Grid dependence research involved selecting a random configuration and changing the element sizes to ensure that each block had at least four subdivisions throughout its entire height and length. The quality of the mesh ranged from 0.937 to 0.972. The computations were completed, and the findings stored. The number of subdivisions was multiplied by 1.3, and the three obtained configurations were compared. The size of the initial time-step allowed a 5° angular sweep of the rotating domain in a single time step. The initial time-step was then modified to finer and coarser values of 2° and 8°, respectively, and the results compared in order to select the sweep angle that decreases computation times and offers trustworthy results. The standard procedure for grid dependence and time-step size analysis is to select an element size and time-step that results in less than 1 % deviation in the value of interest, in this case, the torque, compared to a finer grid

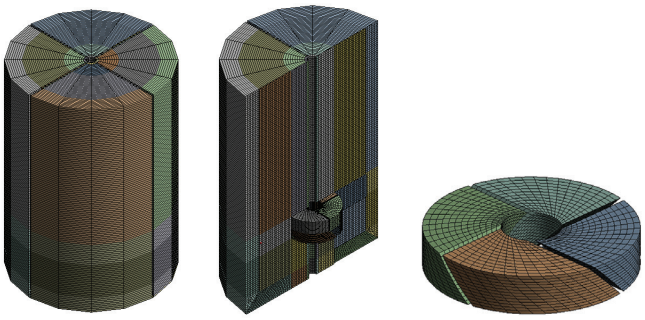

Fig. 2 – Finite volume mesh – baffled reactor: a) isometric view, b) cross-sectional view, and c) magnified finite volume mesh of PBT impeller

Slika 2 – Mreža konačnih volumena – reaktor s razbijalima virova: a) izometrijski prikaz, b) prikaz poprečnog presjeka i c) uvećana mreža konačnih volumena PBT miješala

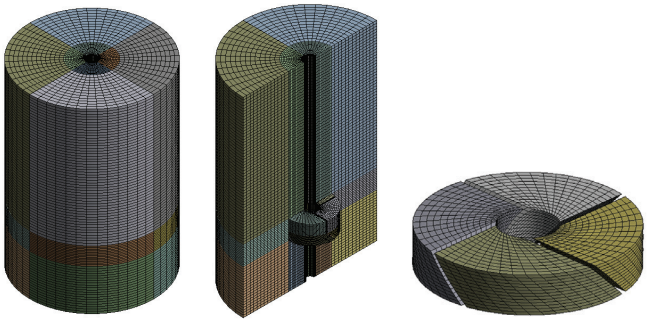

Fig. 3 – Finite volume mesh – unbaffled reactor: a) isometric view, b) cross-sectional view, and c) magnified finite volume mesh of PBT impeller

Slika 3 – Mreža konačnih volumena – reaktor bez razbijala virova: a) izometrijski prikaz, b) prikaz poprečnog presjeka i c) uvećana mreža konačnih volumena PBT miješala

Table 1 – Grid dependency and time-step dependency study for the baffled and unbaffled reactors
Tablica 1 – Utjecaj rezolucije mreže konačnih volumena i veličine vremenskog koraka za reaktore s i bez pregrada

	Baffled batch reactor Šaržni reaktor s razbijalima virova			Unbaffled batch reactor Šaržni reaktor bez razbijala virova		
Configuration Konfiguracija	E1	E2	E3	E1	E2	E3
Number of elements Broj elemenata	82000	181168	404600	90176	123392	255510
Time-averaged torque, N m Vremenski usrednjen zakretni moment, N m	0.0009472	0.0009230	0.0008964	0.0010923	0.0011988	0.0012118
Difference *vs*. finest grid, % Razlika u odnosu na mrežu s najvišom rezolucijom, %	−5.67	−2.97	0.00	9.86	1.07	0.00
	Baffled batch reactor Šaržni reaktor s razbijalima virova			Unbaffled batch reactor Šaržni reaktor bez razbijala virova		
Rotation *per* time-step Rotacija po koraku	2°	5°	8°	2°	5°	8°
Number of elements Broj elemenata	181168			123392		
Time-averaged torque, N m Vremenski usrednjen zakretni moment, N m	0.0009473	0.0009230	0.0008996	0.0011602	0.0011988	0.0010427
Difference *vs*. smallest time-step, % Razlika u odnosu na najmanji korak, %	0.00	−2.57	−5.03	0.00	3.33	−10.13

and a smaller time-step, respectively. However, because of the transient nature of the analyses and the large number of cases analysed, results deviating by less than 5 % from the value of interest were considered sufficient for further system evaluations. The baffled and unbaffled system satisfied this requirement using the E2 grid and 5° rotation per time-step. Table 1 provides information on the mesh test for the impeller used.

2.3 Kinetic experiments

Kinetic studies were conducted at the determined N_{JS}, examining the effect of zeolite mass concentration and baffle presence. The initial concentration of solution, suspension temperature, zeolite particle diameter, and impeller were consistent in all experiments. Samples were taken from the suspension at intervals of up to 30 min to analyse the process kinetics. Following zeolite removal, the copper content was measured using a UV/Vis spectrophotometer

(Lambda 25, Perkin Elmer). The acquired data were used to compute the quantity of copper on the zeolite after sorption, q_t (mmol g^{-1}), and the effectiveness of the process, R_e (%), as follows:

$$q_t = \frac{(c_0 - c_t)\cdot V}{m} \quad (2)$$

$$R_e = \frac{c_0 - c_e}{c_0}\cdot 100 \quad (3)$$

where c_0 is the initial solution concentration (mmol dm^{-3}), c_t (mmol dm^{-3}) is the concentration of the solution at time t, c_e (mmol dm^{-3}) is the concentration of the solution at the end of the experiment, V is the volume of the solution (dm^3), and m is the mass of the synthetic NaX zeolite (g).

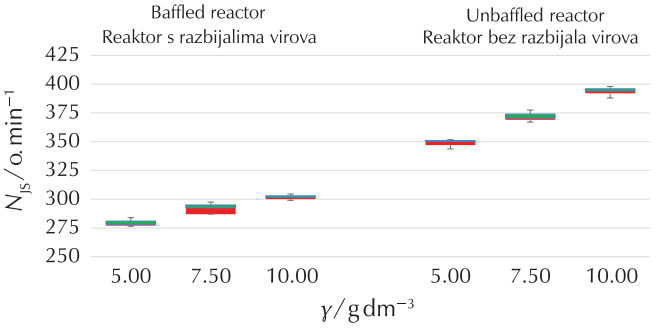

Fig. 4 – *Box plots* – N_{JS} dependence on the zeolite suspension mass concentration in batch reactor

Slika 4 – *Box plots* – Ovisnost brzina N_{JS} o masenoj koncentraciji zeolita NaX u šaržnom reaktoru

3 Results and discussion

3.1 N_{JS}, torque and CFD

Experimentally determined values of the just-suspended impeller speed in the baffled and unbaffled reactors for different zeolite mass suspension concentrations are shown in Fig. 4.

The solid suspension in the batch reactor is strongly influenced by the zeolite mass and baffle presence. As observed in Fig. 4, the N_{JS} increases with higher zeolite mass concentrations. This increase in N_{JS} was expected, as more solids require additional power for suspension.[31] The increase in N_{JS} is more pronounced in the reactor without baffles. Not only is the increase in N_{JS} lower, but the values for the PBT impeller in the reactor with baffles are also lower than those in the reactor without baffles.

This result contrasts with the findings for the same process but with SBT impeller (D/d_T from 0.46 to 0.68). In the study with the SBT impeller located at C/H = 0.33, the increase in zeolite mass led to a more pronounced change in N_{JS} in the reactor with baffles for all impellers used, except the largest one.[29] Furthermore, the N_{JS} values obtained were significantly lower for the unbaffled reactors. However, results from this study align with those obtained when a propeller agitator (D/d_T = 0.46, C/H = 0.33) was used. With the propeller, the increase in N_{JS} with the zeolite mass in the reactor with baffles and even the values of N_{JS} were almost the same as in this study, although the impeller was slightly larger.[26]

This might be related to the results published by *Tamburini et al.*[13] for the Rushton turbine, which indicate that the difference between N_{JS} values in reactors with and without baffles is due to differences in flow patterns produced in those reactors. Thus, the observed similarities and differences might result from the similarities or differences in the flow patterns produced by the SBT, propeller, and PBT impeller. According to the literature[26], propeller agitators typically produce an axial flow, whereas SBT impellers are known to produce a radial fluid flow, although this type of impeller does not pump in a true radial direction due to pressure differences between the two sides of the impeller.[17] PBT impeller is known as a "mixed flow agitator" and its size and location in a baffled reactor will result in a more noticeable axial or radial component of flow.[17,32] The PBT impeller employed in this research develops flow with a prevailing axial component (Fig. 5.). According to the literature, axial flow is more efficient for mixing suspension in solid-liquid systems.[31,33] The impeller's blades direct the suspension to-

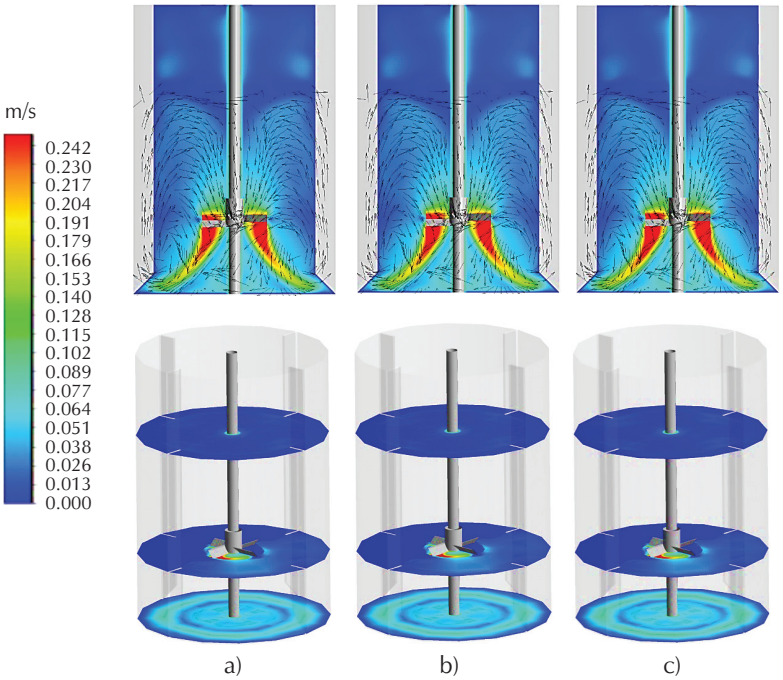

Fig. 5 – Fluid flow and velocities in stationary frame simulation in baffled batch reactor for zeolite mass concentration of: a) 5.00 g dm^{-3}, b) 7.50 g dm^{-3}, and c) 10.00 g dm^{-3}

Slika 5 – Konture tokova i brzina fluida u šaržnom reaktoru opremljenom razbijalima virova za masenu koncentraciju zeolita: a) 5,00 g dm^{-3}, b) 7,50 g dm^{-3} i c) 10,00 g dm^{-3}

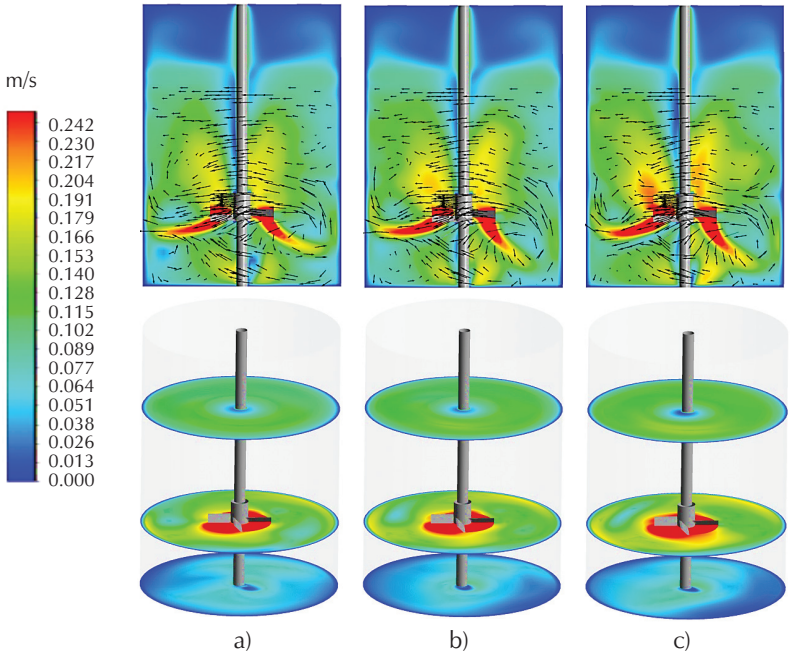

Fig. 6 – Fluid flow and velocities in stationary frame simulation in unbaffled batch reactor for zeolite NaX mass concentration of: a) 5.00 g dm^{-3}, b) 7.50 g dm^{-3}, and c) 10.00 g dm^{-3}

Slika 6 – Konture tokova i brzina fluida u šaržnom reaktoru bez razbijala virova za masenu koncentraciju zeolita NaX: a) 5,00 g dm^{-3}, b) 7,50 g dm^{-3} i c) 10,00 g dm^{-3}

ward the reactor bottom, redirecting it to the reactor walls then the surface, before being pulled back to the impeller. The velocity gradient is prominent around and under the impeller. Higher velocities also occur closer to the reactor bottom, where momentum supports suspension. Despite the simulations in Fig. 5 being performed with N_{JS}, the velocities above the impeller, except along the shaft, are low. This is because the fluid flow returns to the impeller once the suspension reaches a certain height.

In the unbaffled reactor at N_{JS}, it was expected that the suspension would circulate along the axis and move in a circulating path[17], but for the impeller used in this study, a slight deviation from the expected flow was observed at the level and below the impeller, Fig. 6.

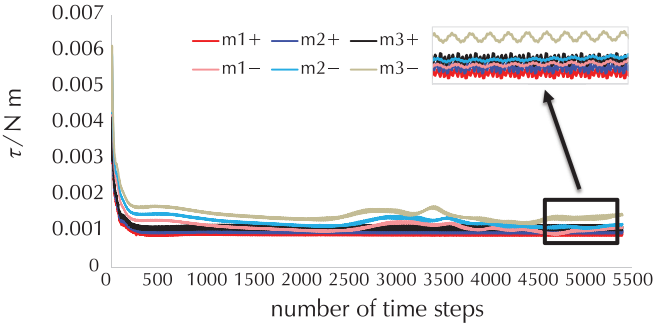

Fig. 7 – Grid and time-step dependency for zeolite mass concentrations used and baffle presence

Slika 7 – Ovisnost masenog udjela zeolita numeričkog proračuna o rezoluciji mreže, vremenskom koraku i prisutnosti razbijala virova

Based on the velocity distribution in the stationary frame simulation (Figs. 5 and 6), it was observed that an increase in the NaX zeolite mass concentration, *i.e.*, an increase in N_{JS}, resulted in an increase in the mixing intensity in the unbaffled reactor. Due to the small differences in critical mixing speeds for given mass concentrations, the increase in mixing intensity was insignificant. In the baffled reactor, the differences in N_{JS} for different masses were even smaller, making the differences in velocities less noticeable.

In addition to simulating fluid flow and velocities in a stationary frame, CFD analysis was employed to calculate the torque, a crucial parameter for power consumption calculation. Fig. 7 shows the findings of the development of the torque over time for all investigated zeolite NaX mass concentrations, both in the baffled and unbaffled reactors, under the specified reaction conditions.

As observed, the results start to repeat themselves after about 800 time steps for all investigated zeolite mass concentrations in the baffled reactor. In the unbaffled reactor, quasi-steady-state was reached after 5100 time steps for all investigated zeolite mass concentrations.

3.2 Kinetic analysis

The experimental data were interpreted using the Ritchie model and the Mixed kinetic model. The Ritchie model is a reaction-based model. Assuming that the reaction is second order, it is expressed as:[34]

$$q_t = q_e\left(1-\frac{1}{1+k_r t}\right) \tag{4}$$

where q_e is the amount of copper on zeolite at equilibrium (mmol g^{-1}), k_r (g mmol^{-1} min^{-1}) is the rate constant, and t is the time (min).

If the rates of diffusion and surface reactions are comparable, the overall kinetic model cannot be reduced to the model of the slowest process. Therefore, the process is represented by mixed models, which incorporate both reaction and diffusion. The Mixed kinetic model, is expressed as:[35]

$$q_t = q_e\frac{e^{\left(a t+b t^{1/2}\right)}-1}{u_e\, e^{\left(a t+b t^{1/2}\right)}-1} \tag{5}$$

where $u_e = 1-(c_e/c_0)$, $a = k\,c_0(u_e-1)$, $b = 2k\,c_0\Psi^{1/2}(u_e-1)$, Ψ is a parameter quantifying the influence of a diffusion process on the reaction rate (min); if $\Psi > 0$ diffusion affects the kinetics.

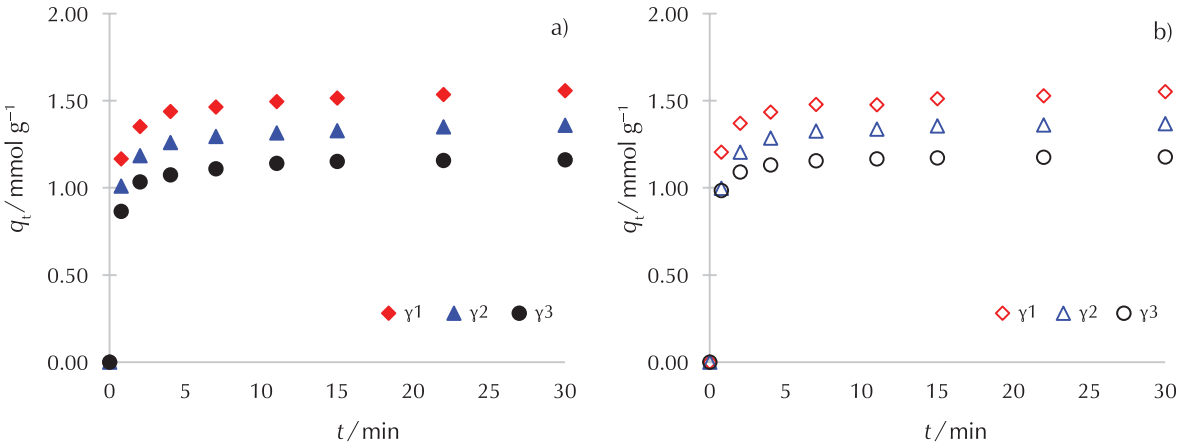

Fig. 8 – Experimetal data in a) baffled batch reactor, and b) unbaffled batch reactor
Slika 8 – Eksperimentalni podatci u šaržnom reaktoru: a) s razbijalima virova b) bez razbijala virova

The nonlinear least square method was used to calculate the model parameters. All calculations were performed using Mathcad (PTC). The degree of fit of the applied kinetic models was assessed by the average absolute relative deviation AARD (%), which is regarded acceptable up to 5 %:[28]

$$\mathrm{AARD} = \frac{1}{n}\sum_{i=1}^{n}\left(\left|\frac{q_{t_i} - q_{t,\mathrm{model}_i}}{q_{t_i}}\right| \cdot 100\right) \qquad (6)$$

where q_t is the experimental value, and $q_{t,\mathrm{model}}$ is the calculated value of q_t.

Fig. 8. shows the kinetic sorption data from the experiments, while Table 2 provides the estimated model parameters. The amount of copper retained per unit mass of zeolite on the NaX zeolite over time, q_t, shows the usual dependence. It increased rapidly in the first few minutes of the kinetic experiments, followed by a decrease in velocity, and the gradual attainment of equilibrium or a near-equilibrium state. Differences in the sorption rate in the initial minutes and throughout the experiment are not only a consequence of the current number of free sorption sites on the NaX zeolite, but also of the concentration gradient value.[36] In the initial phase of the process, the system is characterised by a large concentration gradient and a large number of available free sorption sites on the zeolite.

It is evident that the maximum values of q_t are independent of baffle presence. Regarding the zeolite mass concentration, q_t decreased as the mass concentration of zeolite in the solution increased, because a larger dose of the sorbent contains a greater number of sites available for the sorption of copper. In other words, increasing the mass concentration of zeolite NaX in the solution increases the number of available sorption sites and facilitates the migration of copper to the sorption sites.[37]

Table 2 – Experimental data and estimated kinetics models parameters
Tablica 2 – Eksperimentalni podatci i procijenjeni parametri kinetičkih modela

Reactor with baffles	γ / g dm^{-3}	5.00	7.50	10.00
Experimental data	$q_{e.exp}$ (mmol g^{-1})	1.558	1.359	1.160
	R (%)	64.506	83.953	95.834
	$u_{e.exp}$	0.645	0.840	0.958
Ritchie model	q_e (mmol g^{-1})	1.545	1.353	1.164
	k_r (g mmol^{-1} min^{-1})	3.548	3.770	3.797
	AARD	0.657	0.689	0.614
Mixed kinetic model	q_e (mmol g^{-1})	1.498	1.317	1.153
	u_e	0.682	0.787	0.955
	k (dm^3 mmol^{-1} min^{-1})	0.224	0.259	0.311
	ψ (min)	0.000	0.000	0.000
	AARD	2.036	1.763	0.721
Reactor without baffles	γ / g dm^{-3}	5.00	7.50	10.00
Experimental data	$q_{e.exp}$ (mmol g^{-1})	1.553	1.310	1.177
	R (%)	64.780	80.142	95.695
	$u_{e.exp}$	0.648	0.801	0.957
Ritchie model	q_e (mmol g^{-1})	1.530	1.314	1.182
	k_r (g mmol^{-1} min^{-1})	4.691	6.224	6.464
	AARD	0.942	0.622	0.260
Mixed kinetic model	q_e (mmol g^{-1})	1.489	1.289	1.171
	u_e	0.619	0.779	0.952
	k (dm^3 mmol^{-1} min^{-1})	0.266	0.367	0.498
	ψ (min)	0.000	0.000	0.000
	AARD	2.155	1.580	0.553

For all experiments in this study using the Ritchie model, the calculated values of the maximum sorption capacity, q_e, agree very well with the experimentally determined values of the sorption capacity, $q_{e,exp}$, under the specified reaction conditions. As expected, their value decreased with increasing zeolite mass concentration in the solution, given that the total amount of copper ions bound to zeolite NaX per unit mass of zeolite was lower in the experiments with higher zeolite NaX mass concentration.

The Mixed kinetic model provided a lower agreement of q_e and $q_{e,exp}$. Additionally, for this model, parameter Ψ needs to be taken into account, as its value reveals the influence of diffusion on the kinetics of sorption. According to the literature, if the parameter Ψ is greater than zero minutes, diffusion affects the overall speed of the sorption process.[35]

To further assess the level of agreement between the Ritchie and Mixed kinetic models with the experimental kinetic data, the AARD values were also calculated. The data presented in Table 2 exhibit better agreement with the Ritchie model.

The rate constant increases with the increase in zeolite NaX mass concentration in both the Ritchie and Mixed kinetic models, which is an expected trend as a greater number of sorption centres are available throughout the duration of the experiment.[37]

3.3 Effectiveness of sorption

The next step was to determine the power consumption, as the appropriate hydrodynamic parameters could not be determined without understanding how they affect the cost and kinetics of the process. However, not only is power consumption important, but also its relationship with the rate constant and sorption efficiency. These relationships are presented in Figs. 9 and 10.

The presence of baffles and the power consumption had no influence on the efficiency of sorption for all mass concentrations of zeolite used. However, it is evident that the power consumption was higher in the system without baf-

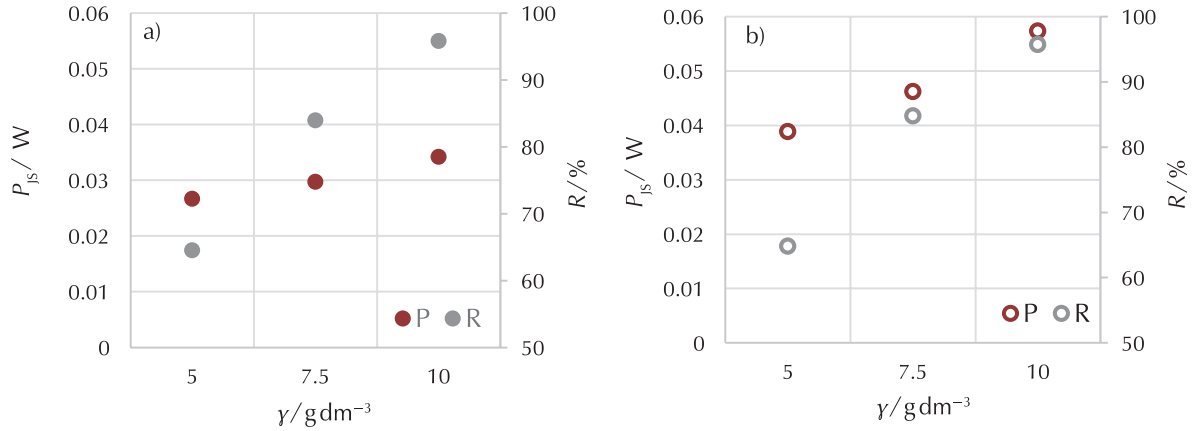

Fig. 9 – Dependence of power consumption and sorption efficiency on zeolite mass concentration in: a) baffled batch reactor, and b) unbaffled batch reactor

Slika 9 – Ovisnost utroška snage i učinkovitosti sorpcije o masenoj koncentraciji zeolita u šaržnom reaktoru: a) s razbijalima virova i b) bez razbijala virova

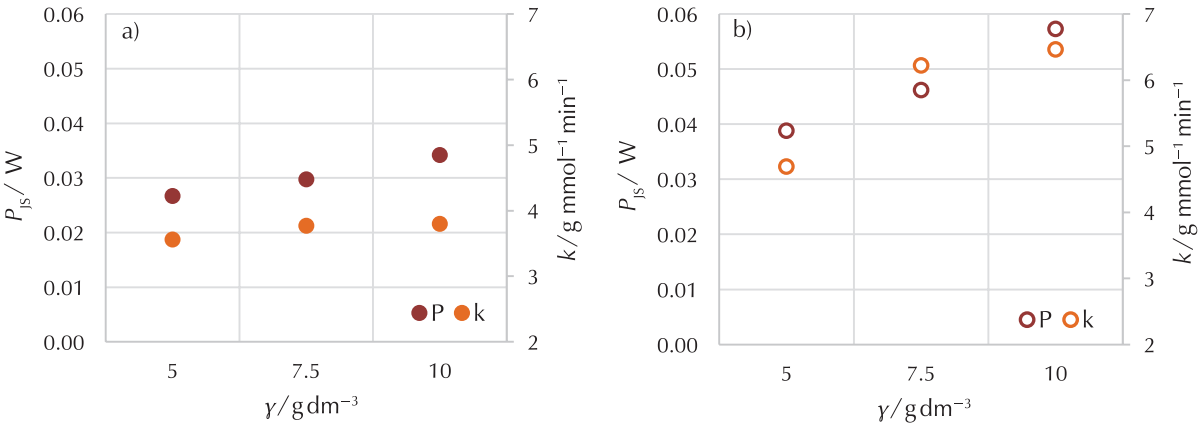

Fig. 10 – Dependence of power consumption and Ritchie rate constant on zeolite concentration in: a) baffled batch reactor, and b) unbaffled batch reactor

Slika 10 – Ovisnost utroška snage i konstante brzine Richiejevog modela o koncentraciji zeolita u šaržnom reaktoru: a) s razbijalima virova i b) bez razbijala virova

fles. Regarding the dependence of the sorption rate constant of the Ritchie model and power consumption on the mass concentration of the zeolite in a batch reactor with and without baffles, the results presented clearly show that both power consumption and the sorption rate constant of the Ritchie model are higher in the batch reactor without baffles.

4 Conclusion

After conducting the copper sorption process on NaX zeolite particles with a size class smaller than 90 μm, at three different zeolite NaX mass concentrations ($\gamma_1 = 5.00\ \mathrm{g\,dm^{-3}}$, $\gamma_2 = 7.50\ \mathrm{g\,dm^{-3}}$ and $\gamma_3 = 10.00\ \mathrm{g\,dm^{-3}}$), both in the presence and absence of baffles, under isothermal conditions (25 °C), the following conclusions can be drawn:

An increase in zeolite mass concentration leads to a higher N_{JS} rate, resulting in increased energy consumption in both baffled and unbaffled reactors.

Considering the low AARD values when comparing the experimental kinetic data with Ritchie's model, it can be concluded that the process of copper sorption on NaX zeolite can be described very well by Ritchie's kinetic model. This suggests that it is a second-order reaction under the studied reaction conditions.

The presence of baffles had no significant effect on the amount of copper sorbed or on the efficiency of the tested process. However, the presence of baffles led to a reduction in power consumption and reaction speed, as a lower speed was required to reach a state of complete suspension in this system, which generally affects power consumption and homogenisation mixing time.

ACKNOWLEDGEMENTS

We express gratitude for the scientific-research equipment and computer programme financed by EU grant "Functional Integration of the University of Split, PMF-ST, PFST, and KTFST through the Development of Scientific and Research Infrastructure" (KK.01.1.1.02.0018), and project STIM–REI (contract number: KK.01.1.1.01.0003), funded by the European Union through the European Regional Development Fund – Operational Programme Competitiveness and Cohesion 2014-2020 (KK.01.1.1.01.)

List of abbreviations and symbols
Popis kratica i simbola

AARD – average absolute relative deviation, %
– srednje apsolutno relativno odstupanje, %

ψ – Mixed kinetic model parameter, min
– parametar Miješanog kinetičkog modela, min

a – Mixed kinetic model parameter
– parametar Miješanog kinetičkog modela

b – Mixed kinetic model parameter
– parametar Miješanog kinetičkog modela

C – impeller clearance, m
– udaljenost miješala od dna posude, m

C/H – off-bottom clearance
– omjer udaljenosti miješala od dna posude i visine stupca kapljevine

c_0 – initial solution concentration, $\mathrm{mmol\,dm^{-3}}$
– početna koncentracija otopine, $\mathrm{mmol\,dm^{-3}}$

c_e – concentration of the solution at the end of the experiment, $\mathrm{mmol\,dm^{-3}}$
– koncentracija otopine na kraju eksperimenta, $\mathrm{mmol\,dm^{-3}}$

c_t – concentration of the solution at time t, $\mathrm{mmol\,dm^{-3}}$
– koncentracija otopine u trenutku t, $\mathrm{mmol\,dm^{-3}}$

D – impeller diameter, m
– promjer miješala, m

D/d_T – impeller diameter to inner reactor diameter ratio
– omjer promjera miješala i unutarnjeg promjera reaktora

d_p – particle diameter of NaX zeolite, m
– promjer čestica zeolita NaX, m

d_T – inner reactor diameter, m
– promjer reaktora, m

H – liquid height, m
– visina stupca kapljevine, m

k – Mixed kinetic model constant rate, $\mathrm{g\,mmol^{-1}\,min^{-1}}$
– konstanta brzine Miješanog kinetičkog modela, $\mathrm{g\,mmol^{-1}\,min^{-1}}$

k_r – Ritchie model constant rate, $\mathrm{g\,mmol^{-1}\,min^{-1}}$
– konstanta brzine Richiejevog modela, $\mathrm{g\,mmol^{-1}\,min^{-1}}$

N – impeller mixing speed, rpm
– brzina vrtnje miješala, $\mathrm{o\,min^{-1}}$

N_{JS} – just suspended impeller speed, rpm
– kritična brzina vrtnje miješala, $\mathrm{o\,min^{-1}}$

P_{JS} – mixing power consumption at N_{JS}, W
– utrošak snage miješanja pri N_{JS}, W

q_e – amount of copper on zeolite at equilibrium, $\mathrm{mmol\,g^{-1}}$
– količina sorbirane tvari u ravnoteži, $\mathrm{mmol\,g^{-1}}$

q_t – amount of copper on zeolite at time t, $\mathrm{mmol\,g^{-1}}$
– količina sorbirane tvari u trenutku t, $\mathrm{mmol\,g^{-1}}$

R_v – baffles width, m
– širina razbijala virova, m

T – temperature, °C
– temperatura, °C

t – time, min
– vrijeme, min

u_e – Mixed kinetic model parameter
– parametar Miješanog kinetičkog modela

V – solution volume, $\mathrm{dm^3}$
– volumen otopina, $\mathrm{dm^3}$

α – angle between baffles and reactor bottom, °
– kut između razbijala virova i dna reaktora, °

γ – zeolite mass concentration in the solution, $\mathrm{g\,dm^{-3}}$
– masena koncentracija zeolita u otopini, $\mathrm{g\,dm^{-3}}$

τ – torque, N m
– zakretni moment, N m

References
Literatura

1. *A. Bašić, M. N. Mužek, L. Kukoč Modun, S. Svilović*, Competitive heavy metal removal from binary solution, Kem. Ind. **69** (2020) 465–471, doi: https://doi.org/10.15255/KUI.2020.038.
2. *S. Svilović, N. Vukojević Medvidović, L. Vrsalović, A. Kulić*, Combining natural zeolite and electrocoagulation with different electrode materials – electrode surface analysis and Taguchi optimization, Applied Surf. Sci. Adv. **12** (2022) 100330, doi: https://doi.org/10.1016/j.apsadv.2022.100330.
3. *Y. Fei, Y. H. Hu*, Recent progress in removal of heavy metals from wastewater: A comprehensive review, Chemosphere **335** (2023) 139077, doi: https://doi.org/10.1016/j.chemosphere.2023.139077.
4. *L. Vrsalović, N. Vukojević Medvidović, S. Svilović, J. Šarić,* Application of Different Metals as Electrode Material in Compost Leachate Treatment, Kem. Ind. **72** (2023) 297–304. doi: https://doi.org/10.15255/KUI.2022.066.
5. *H. A. Hegazi*, Removal of heavy metals from wastewater using agricultural and industrial wastes as adsorbents, HBRC Journal **9** (2013) 276–282, doi: https://doi.org/10.1016/j.hbrcj.2013.08.004.
6. *S. E. Bailey, T. J. Olin, R. M. Bricka, D. D. Adrian*, A review of potentially low-cost sorbents for heavy metals, Water Res. **33** (1999) 2469–2479, doi: https://doi.org/10.1016/s0043-1354(98)00475-8.
7. *K. Kadirvelu, K. Thamaraiselvi, C. Namasivayam*, Removal of heavy metals from industrial wastewaters by adsorption onto activated carbon prepared from an agricultural solid waste, Bioresour. Technol. **76** (2001) 63–65, doi: https://doi.org/10.1016/s0960-8524(00)00072-9.
8. *J. Hoslett, H. Ghazal, D. Ahmad, H. Jouhara*, Removal of copper ions from aqueous solution using low temperature biochar derived from the pyrolysis of municipal solid waste, Sci. Total Environ. **673** (2019) 777–789, doi: https://doi.org/10.1016/j.scitotenv.2019.04.085.
9. *T. C. Nguyen, P. Loganathan, T. V. Nguyen, J. Kandasamy, R. Naidu, S. Vigneswaran,* Adsorptive removal of five heavy metals from water using blast furnace slag and fly ash, Environ. Sci. Pollut. Res. **25** (2018) 20430–20438, doi: https://doi.org/10.1007/s11356-017-9610-4.
10. *S. Svilović, D. Rušić, A. Bašić,* Investigations of different kinetic models of copper ions sorption on zeolite 13X, Desalination **259** (2010) 71–75, doi: https://doi.org/10.1016/j.desal.2010.04.033.
11. *V. Singh, J. Singh, V. Mishra,* Development of a cost-effective, recyclable and viable metal ion doped, adsorbent for simultaneous adsorption and reduction of toxic Cr (VI) ions, J. Environ. Chem. Eng. **9** (2021) 105124, doi: https://doi.org/10.1016/j.jece.2021.105124.
12. *A. W. Nienow,* Suspension of solid particles in turbine agitated baffled vessels, Chem. Eng. Sci. **23** (1968) 1453–1459, doi: https://doi.org/10.1016/0009-2509(68)89055-4.
13. *A. Tamburini, A. Cipollina, G. Micale, A. Brucato*, Measurements of N_{js} and Power Requirements in Unbaffled Bioslurry Reactors, Chem. Eng. Trans. **27** (2012) 343–348, doi: https://doi.org/10.3303/CET1227058.
14. *R. Jafari, P. A. Tanguy, J. Chaouki,* Characterization of minimum impeller speed for suspension of solids in liquid at high solid concentration, using gamma-ray densitometry, Int. J. Chem. Eng. (2012) 945314, doi: https://doi.org/10.1155/2012/945314.
15. *G. Baldi, R. Conti, E. Alaria*, Complete suspension of particles in mechanically agitated vessels, Chem. Eng. Sci. **33** (1978) 21–25, doi: https://doi.org/10.1016/0009-2509(78)85063-5.
16. *S. Svilović, I. Horvat, M. Ćosić, R. Stipišić*, Investigation on the effects of process variables on copper exchange on NaX in a batch stirred reactor, Teh. Glas. **11** (2017) 171–174, url: https://hrcak.srce.hr/190995.
17. *E. I. Paul, V. A. Atiemo-Obeng, S. M Kresta* (Eds.), Handbook of Industrial Mixing, John Wiley & Sons, Inc., Hoboken, New Jersey, 2003, pp. 345–390, doi: https://doi.org/10.1002/0471451452.ch6.
18. *M. Jaszczur, A. Mlynarczykowska*, A General Review of the Current Development of Mechanically Agitated Vessels, Processes **8** (2020) 982, doi: https://doi.org/10.3390/pr8080982.
19. *A. Busciglio, F. Grisafi, F. Scargiali, A. Brucato*, Mixing dynamics in uncovered unbaffled stirred tanks, Chem. Eng. J. **254** (2014) 210–219, doi: https://doi.org/10.1016/j.cej.2014.05.084.
20. *A. Tamburini, A. Cipollina, G. Micale, A. Brucato*, Particle distribution in dilute solid liquid unbaffled tanks *via* a novel laser sheet and image analysis based technique, Chem. Eng. Sci. **87** (2013) 341–358, doi: https://doi.org/10.1016/j.ces.2012.11.005.
21. *A. Brucato, A. Cipollina, G. Micale, F. Scargiali, A. Tamburini*, Particle suspension in top-covered unbaffled tanks, Chem. Eng. Sci. **65** (2010) 3001–3008, doi: https://doi.org/10.1016/j.ces.2010.01.026.
22. *F. Scargiali, A. Busciglio, F. Grisafi, A. Tamburini, G. Micale, A. Brucato*, Power Consumption in Uncovered Unbaffled Stirred Tanks: Influence of the Viscosity and Flow Regime, Ind. Eng. Chem. Res. **52** (2013) 14998–15005, doi: https://doi.org/10.1021/ie402466w.
23. *I. Sreedhar, N. Saketharam Reddy*, 2019. Heavy metal removal from industrial effluent using bio-sorbent blends, SN Appl. Sci. **1** (2019) 1021, doi: https://doi.org/10.1007/s42452-019-1057-4.
24. *N. Vukojević Medvidović, S. Svilović*, Cyclic zinc capture and zeolite regeneration using a column method, mass transfer analysis of multi regenerated bed, J. Environ. Health Sci. Eng. **21** (2023) 333–353, doi: https://doi.org/10.1007/s40201-023-00861-2.
25. *A. Bašić, Ž. Penga, M. N. Mužek, S. Svilović,* Impact of turbine impeller blade inclination on the batch sorption process. Results Eng. 1**6** (2022) 100554, doi: https://doi.org/10.1016/j.rineng.2022.100554.
26. *A. Bašić, Ž. Penga, J. Penga, N. Kuzmanić, S. Svilović,* Zeolite NaX mass and propeller agitator speed impact on copper ions sorption, Processes **11** (2023) 264, doi: https://doi.org/10.3390/pr11010264.
27. *D. Chitra, L. Muruganandan*, Effect of Solid concentration and impeller type on Mixing Operation in an Agitated Vessel, Int. J. Chem Tech Res. **6** (2014) 3665–3671.
28. *A. Bašić, S. Svilović*, Effect of geometrical and operating mixing parameters on copper adsorption on zeolite NaX, Desalin. Water Treat. **209** (2021) 197–203, doi: https://doi.org/10.5004/dwt.2021.26524.
29. *S. Svilović, M. Ćosić, A. Bašić*, Effect of radial impeller size in the presence and absence of baffles on the copper exchange on zeolite NaX, Eng. Rev. **41**(2) (2021) 125–135, doi: https://doi.org/10.30765/er.1574.
30. *Th. N. Zwietering*, Suspending of solid particles in liquid by agitators, Chem. Eng. Sci. **8** (1958) 244–253, doi: https://doi.org/10.1016/0009-2509(58)85031-9.
31. *R. Jafari, P. A. Tanguy, J. Chaouki*, Characterization of min-

imum impeller speed for suspension of solids in liquid at high solid concentration using gamma-ray densitometry. Int. J. Chem. Eng. **2012** (2012) 945314, doi: https://doi.org/10.1155/2012/945314.

32. *N. Harnby, M. F. Edwards, A. W. Nineow*, Mixing in the Process Industries, 2nd ed.; Butterworth-Heinemann, Oxford, UK, 1992; pp. 377.
33. *K. S. M. S. Raghav Rao, J. B. Joshi*, Liquid-phase Mixing and Power Consumption in Mechanically Agitated Solid-Liquid Contactors, The Chemical Engineering Journal **39** (1988) 111–124, doi: https://doi.org/10.1016/0300-9467(88)80101-1.
34. *A. G. Ritchie*, Alternative to Elovich equation for the kinetics of adsorption of gasses on solids, J. Chem. Soc. Faraday Trans. 1 **73** (1977) 1650–1653, doi: https://doi.org/10.1039/F19777301650.
35. *M. Haerifar, S. Azizian*, Mixed surface reaction and diffusion-controlled kinetic model for adsorption at the solid/solution interface, J. Phys. Chem. C **117** (2013) 8310–8317, doi: https://doi.org/10.1021/jp401571m.
36. *N. Bakhtiari, S. Azizian*, Adsorption of copper ion from aqueous solution by nanoporous MOF-5: a kinetic and equilibrium study, J. Mol. Liq. **206** (2015) 114–118, https://doi.org/10.1016/j.molliq.2015.02.009.
37. *G. Buema, L.-M. Trifas, M. Harja*, Removal of Toxic Copper Ion from Aqueous Media by Adsorption on Fly Ash-Derived Zeolites: Kinetic and Equilibrium Studies, Polymers **13** (2021) 3468, doi: https://doi.org/10.3390/polym13203468.

SAŽETAK

Utjecaj mase NaX zeolita i uporabe razbijala virova na sorpciju bakra

Ana Herceg,[a] *Anita Bašić*,[a*] *Željko Penga*[b] i *Sandra Svilović*[a]

Sorpcija se često provodi u šaržnom reaktoru s miješanjem bez procjene utjecaja miješanja na prinos i troškove. Izvođenje miješanja u šaržnom reaktoru u stanju potpune suspenzije, tj. pri minimalnoj brzini vrtnje miješala potrebnoj za postizanje stanja potpune suspenzije, N_{JS}, kompromis je između navedenih ciljeva. Zato je sorpcija bakra na NaX zeolitu provedena pomoću turbinskog miješala s ravnim lopaticama nagnutim pod kutom od 45° (PBT miješalo) u šaržnom reaktoru s razbijalom i bez razbijala virova pri N_{JS} brzinama. Omjer promjera PBT miješala i unutarnjeg promjera šaržnog reaktora ($D/d_T = 0{,}32$), kao i omjer udaljenosti miješala od dna reaktora i visine suspenzije, ($C/H = 0{,}33$) bili su konstantni. Osim kinetičkih sorpcijskih eksperimenata i kinetičke analize dobivenih podataka, provedene su i prijelazne višefazne računske simulacije dinamike fluida (CFD), da bi se dobio uvid u hidrodinamičko ponašanje sustava.

Brzina N_{JS} povezana je s brzinom taloženja čestica, stoga veća masena koncentracija suspenzije zeolita zahtijeva veću brzinu N_{JS} i utrošak energije. Razlike u brzinama N_{JS} za ispitivane masene koncentracije suspenzije zeolita nisu velike, pa stoga povećanje intenziteta miješanja za ispitane sustave nije značajno. Utvrđeno je da su vrijednosti N_{JS} i P_{JS} (utrošak snage miješanja) veće u reaktoru bez razbijala virova bez obzira na upotrijebljenu masu zeolita. Primijenjeni hidrodinamički uvjeti ne utječu znatno na maksimalnu količinu sorbiranog bakra niti na učinkovitost procesa, ali na navedeno znatno utječe masa zeolita. Na kinetiku utječe i masa zeolita i primijenjeni hidrodinamički uvjeti, a općenito je brža u reaktoru bez razbijala virova.

Ključne riječi
Kinetika sorpcije, bakar, masena koncentracija zeolita, razbijala virova, CFD

[a] *Sveučilište u Splitu, Kemijsko-tehnološki fakultet, Ruđera Boškovića 35, 21 000 Split*
[b] *Sveučilište u Splitu, Fakultet elektrotehnike, strojarstva i brodogradnje, Ruđera Boškovića 32, 21 000 Split*

Izvorni znanstveni rad
Prispjelo 29. rujna 2023.
Prihvaćeno 29. studenoga 2023.